Ortho metalation of pyridine at a diiridium center. Synthesis and spectroscopic and crystallographic characterization of NC5H4- and N,N'-di-p-tolylformamidinato-bridged complexes of diiridium(II)

F. Albert Cotton, Rinaldo Poli

Ortho Metalation of Pyridine at a Diiridium Center. Synthesis and Spectroscopic and Crystallographic Characterization of NC_5H_4- and *N,N'*-Di-*p*-tolylformamidinato-Bridged Complexes of Diiridium(II)

F. Albert Cotton* and Rinaldo Poli

Department of Chemistry and Laboratory for Molecular Structure and Bonding, Texas A&M University, College Station, Texas 77843

Received January 29, 1987

The compound (COD)Ir(μ-form)$_2$Ir(OCOCF$_3$)$_2$(H$_2$O) (1) (COD = 1,5-cyclooctadiene; Hform = *N,N'*-di-*p*-tolylformamidine) thermally activates pyridine under mild conditions to afford the ortho-metalated derivative [Ir$_2$(μ-NC$_5$H$_4$)$_2$(μ-form)(py)$_4$]$^+$OCOCF$_3^-$ (3) in high yields. Metathesis with NaBPh$_4$ in MeCN affords [Ir$_2$(μ-NC$_5$H$_4$)$_2$(μ-form)(py)$_2$(MeCN)$_2$]$^+$BPh$_4^-$ (4). The cations in compounds 3 and 4 contain a singly bonded diiridium(II) core bridged by one form and two NC$_5$H$_4$ groups and bonded to two equatorial pyridine ligands. Axial pyridine (for 3) and MeCN (for 4) ligands complete the coordination sphere. Compound 4 crystallizes with two interstitial MeCN molecules. Crystal data: triclinic, space group $P\bar{1}$, a = 17.934 (5) Å, b = 18.397 (6) Å, c = 9.652 (1) Å, α = 97.09 (2)°, β = 97.67 (2)°, γ = 76.71 (2)°, V = 3057 (2) Å^3, d_{calcd} = 1.527 g·cm^{-3}, Z = 2, R = 0.0435 (R_w = 0.0518) for 4446 data having $F_o^2 > 3\sigma(F_o^2)$. The iridium–iridium distance, 2.517 (1) Å, is the shortest ever reported.

Introduction

We recently reported[1] that the oxidation of the formamidinato-bridged dimer of iridium(I) [Ir(form)(COD)]$_2$ [Hform = *N,N'*-di-*p*-tolylformamidine; COD = 1,5-cyclooctadiene) with AgOCOCF$_3$ results in the formation of the diiridium(I,III) compound (COD)Ir(μ-form)$_2$Ir(OCOCF$_3$)$_2$(H$_2$O) (1) containing a dative metal–metal bond. This result is in contrast with the reported[2] analogous reaction of the rhodium system, where the homogeneous-valence Rh(II) dimer Rh$_2$(μ-form)$_2$(μ-OCOCF$_3$)$_2$ is obtained in a number of adducts with different axial ligands. We also reported[1] that compound 1 easily exchanges its axially coordinated water molecule with neutral ligands and the pyridine adduct (COD)Ir(μ-form)$_2$Ir(OCOCF$_3$)$_2$py (2) was crystallographically characterized. During such a ligand exchange reaction we observed the formation of an orange powder along with the dark red crystals of compound 2.[1] We conjectured that such a material might be a homogeneous-valence iridium(II) dimer with bridging formamidinate and trifluoroacetate groups, analogous to the reported[2] rhodium complex. We therefore investigated the reaction between 1 and pyridine

(1) Cotton, F. A.; Poli, R. *Inorg. Chem.* **1987**, *26*, 590.
(2) Piraino, P.; Bruno, G.; Tresoldi, G.; Lo Schiavo, S.; Zanello, P. *Inorg. Chem.* **1987**, *26*, 91.

in more detail, and we report here our findings.

Experimental Section

All operations were carried out in standard Schlenkware under an atmosphere of prepurified argon. Solvents were purified by conventional methods and distilled under dinitrogen prior to use. Instruments used were as follows: Perkin-Elmer 783 (IR), Varian XL-200 (^{1}H and ^{13}C NMR), Varian XL-400 (^{19}F NMR). Elemental analyses were by Galbraith Laboratories Inc., Knoxville, TN. The compound (COD)Ir(μ-form)$_2$Ir(OCOCF$_3$)$_2$(H$_2$O)·C$_6$H$_{14}$ (**1**·C$_6$H$_{14}$) was prepared as previously described.[1]

Synthesis of [Ir$_2$(μ-NC$_5$H$_4$)$_2$(μ-form)(py)$_4$]$^+$OCOCF$_3^-$·py (3·py). Compound **1**·C$_6$H$_{14}$ (0.26 g, 0.21 mmol) was dissolved in 5 mL of pyridine to give a dark red solution. This was treated with 20 mL of *n*-hexane, and the resulting solution was warmed without stirring at 60 °C. The color of the solution turned to pale orange, and well-formed orange crystals of **3**·py formed on the walls of the Schlenk tube within $^1/_2$ h. The product was decanted, washed with *n*-hexane, and dried *in vacuo*; yield 0.20 g (74%). The temperature was found to be critical for this reaction, as a lower temperature afforded the product but as a very impure oily material. A higher temperature, although not affecting the nature of the product, caused the formation of smaller crystals. Anal. Calcd for C$_{52}$H$_{48}$F$_3$Ir$_2$N$_9$O$_2$: C, 49.1; H, 3.8; F, 4.5;, N, 9.9. Found: C, 48.7; H, 3.7; F, 5.4; N, 9.6. IR (Nujol mull, cm^{-1}): 1690 vs, 1580 m, 1540 s, 1500 s, 1480 m, 1445 s, 1415 w, 1360 m, 1220 m, 1200 m, 1155 m, 1115 m, 760 m, 750 m, 655 m. ^{1}H NMR (CH$_2$Cl$_2$, δ): 8.4–6.5 (aromatic, 42 H), 2.26 (s, CH_3, 3 H), 2.24 (s, CH_3, 3 H). ^{19}F NMR (CH$_2$Cl$_2$, δ, downfield of the external standard C$_6$H$_5$CF$_3$): −10.71. ^{13}C NMR spectroscopic properties are reported in Table I.

Compound **3** is soluble in pyridine and CH$_2$Cl$_2$, it reacts with MeCN (vide infra), and it is quickly decomposed by CHCl$_3$. It is stable in refluxing pyridine.

Synthesis of [Ir$_2$(μ-NC$_5$H$_4$)$_2$(μ-form)(py)$_2$(MeCN)$_2$]$^+$-BPh$_4^-$·2MeCN (4·2MeCN). Compound **3**·py (0.13 g, 0.10 mmol) was dissolved in MeCN (5 mL) and treated with an excess (ca. 0.20 g) of NaBPh$_4$. The resulting solution was cooled to −20 °C. Yellow-orange crystals formed in about a week; yield 0.11 g (74%). Anal. Calcd for C$_{67}$H$_{65}$BIr$_2$N$_{10}$: C, 57.2; H, 4.7; N, 10.0. Found: C, 58.0; H, 4.8; N, 9.8. ^{1}H NMR (CH$_2$Cl$_2$, δ): 8.2–6.5 (aromatic, 47 H), 2.38 (s, C$_6$H$_4$CH_3, 3 H), 2.31 (s, C$_6$H$_4$CH_3, 3 H), 2.03 (s, CH_3CN, 12 H). ^{13}C NMR spectroscopic properties are reported in Table I. Compound **4** is soluble in MeCN and CH$_2$Cl$_2$ and is decomposed by CHCl$_3$.

X-ray Crystallography. Compound 3·py. A plate-shaped crystal of dimensions 0.1 × 0.3 × 0.5 mm was sealed under argon in a thin-walled capillary and mounted on a computer-controlled Nicolet P3 diffractometer equipped with graphite-monochromatized Mo Kα radiation (λ = 0.710 73 Å). The crystals are monoclinic, space group $P2_1/n$ (from systematic extinctions), and the lattice parameters, determined by a least-squares calculation based on the setting angles of 25 reflections with $20 < 2\theta < 25°$, are a = 9.691 (3) Å, b = 28.681 (11) Å, c = 17.612 (7) Å, β = 93.46 (3)°, V = 4886 (5) Å^3, d_{calcd} = 1.73 g·cm^{-3}, and Z = 4. Data were collected up to 2θ = 45° with the ω-scan technique. A total of 4472 reflections were measured, of which only 3030, having $F_o^2 > 3\sigma(F_o^2)$, were kept. Data were corrected for Lorentz, polarization, and absorption[3] effects. The transmission factors were in the range 0.99–0.77. The structure was solved by Patterson analysis, which revealed the positions of the heavy atoms, and refined by alternate full-matrix least-squares cycles and difference Fourier maps performed with the Enraf-Nonius SDP software. This led to the correct development of the diiridium cation. At this stage two separate areas in the asymmetric unit not occupied by the diidirium cation showed the presence of peaks in the difference Fourier map. These were interpreted as the trifluoroacetate anion and the pyridine lattice molecule. We could not, however, find a clear assignment of these peaks. The situation did not improve after a further absorption correction according to the method of Walker and Stuart.[4] We concluded that the trifluoroacetate ion and the pyridine molecule are disordered and probably are also subject to high thermal motion. We were not able to find a reasonable model for this disorder, and our isotropic refinement converged at R = 8.90% (R_w = 11.0%). The positional and isotropic thermal parameters for the cation of compound **3**·py have been deposited as supplementary material.

Table I. ^{13}C NMR Spectra of Compounds 3·py and 4·2MeCN (δ [J_{C-B}/Hz])

3·py/CD$_2$Cl$_2$	3·py/py-d_5	4·2MeCN/CD$_2$Cl$_2$	
168.09	168.65	167.51	N–*C*H–N
		164.37 [49.3]	i-BPh$_4$
164.97	165.35	*a*	*o*-metalated NC$_5$H$_4$
162.37	162.85	162.24	
160.15	160.77		*b*
159.54	160.11		
153.42	153.67	154.21	*o*-py (eq)
151.36	150.32	152.94 (*c*)	*o*-py (free + ax.)
150.43	151.06	151.74	i-*C*$_6$H$_4$–CH$_3$
149.81	*d*	151.07	
149.97	*d*	150.74	*o*-py (eq)
147.56	147.73	149.60	6-C
146.04	146.38	146.82	
		136.20 [1.5]	*o*-BPh$_4$
136.33	135.90		*p*-py (free + ax.)
135.90	136.13	135.90	
134.66	134.93	134.94	
133.44	133.24	133.56	*p*-C$_6$H$_4$–CH$_3$
133.06	132.73	132.79	
132.49	132.51	*e*	
131.93	132.04	132.62	
130.41	130.62	130.73	
	130.56	130.49	
129.33	129.65	129.25	*o*-*C*$_6$H$_4$–CH$_3$
129.22	129.55	129.15	
		125.98 [2.7]	*m*-BPh$_4$
126.05	126.50	125.45	*m*-py (eq)
125.26	125.58	124.84	*m*-C$_6$H$_4$–CH$_3$
125.12	125.37		
125.00	124.15	124.51	*m*-py (eq)
124.69	123.90		*m*-py (free + ax.)
		122.06 [<1]	*p*-BPh$_4$
118.10	118.22	118.26	
117.22	117.48	117.39	
		113.56	CH$_3$–*C*N
20.77	20.88	20.87	C$_6$H$_4$–*C*H$_3$
20.70		20.75	
		2.96	*C*H$_3$–CN

[a] Peak probably overlapped with the quartet of i-BPh$_4$. [b] OCOCF$_3$ (?), see text. [c] Impurity (see text). [d] Peak probably overlapped with the peaaks of free py and py-d_5. [e] Peak probably overlapped with the stronger peak at 133.56 ppm.

Compound 4·2MeCN. Data collection and reduction and the solution and refinement of the structure were performed in a similar way to that described above for compound **3**. Crystallographic data are assembled in Table II. All parameters were refined independently, with the exception of the site occupancy factors of the atoms of the bridging ortho-metalated pyridine rings that are bonded to the iridium atoms.

As will be fully discussed later, the question of the relative orientation (head-to-head, HH, or head-to-tail, HT) of the two ortho-metalated pyridine rings is a very critical one. The refinement of the structure was conducted in such a way as to see how much information on this question could be obtained by comparing the behavior of several models under refinement. Four different models were considered. In the first one, an ordered HH model, the two atoms bonded to Ir1 were treated as pure nitrogen atoms and those bonded to Ir2 as pure carbon atoms. The second model, the alternative, ordered HH model, had pure carbon atoms on Ir1 and pure nitrogen atoms on Ir2. In the third, all four atoms were treated as 50% N and 50% C. This is equivalent to either a 1:1 mixture of the two HH models or a 1:1 mixture of the two possible HT orientations. Each of these may be denoted as a constrained disorder model (that is, with the two contributing orientations being required to have equal populations). Finally, two atoms were treated as xN + (1 − x)C and the

(3) North, A. C. T.; Phillips, D. C.; Mathews, F. C. *Acta Crystallogr., Sect. A: Cryst. Phys., Diffr., Theor. Gen. Crystallogr.* **1968**, *A24*, 351.
(4) Walker, N.; Stuart, D. *Acta Crystallogr., Sect. A: Found. Crystallogr.* 1983, *A39*, 158.

Table II. Crystal Data for $[Ir_2(\mu\text{-}NC_5H_4)_2(\mu\text{-form})(py)_2(MeCN)_2][BPh_4]\cdot 2MeCN$

formula	$C_{67}H_{65}BIr_2N_{10}$
fw	1405.54
space group	$P\bar{1}$
systematic absences	none
a, Å	17.934 (5)
b, Å	18.397 (6)
c, Å	9.652 (1)
α, deg	97.09 (2)
β, deg	97.67 (2)
γ, deg	76.71 (2)
V, Å^3	3057 (2)
Z	2
d_{calcd}, g/cm^3	1.527
cryst size, mm	0.3 × 0.5 × 0.1
μ(Mo Kα), cm^{-1}	43.780
data collctn instrument	CAD-4
radiatn (monochromated in incident beam)	Mo Kα (λ_α = 0.710 73 Å)
orientatn reflctns, no. range (2θ)	25, 15–25
temp, °C	20
scan method	ω
data collectn range, 2θ, deg	4–45
no. of unique data, total with $F_o^2 > 3\sigma(F_o^2)$	8262, 4446
no. of parameters refined	723
trans factors, max, min	0.999, 0.817
R^a	0.0435
$R_w{}^b$	0.0518
quality-of-fit indicator^c	1.323
largest shift/esd, final cycle	0.127
largest peak, e/Å^3	1.56

$^a R = \sum||F_o| - |F_c||/\sum|F_o|$. $^b R_w = [\sum w(|F_o| - |F_c|)^2/\sum w|F_o|^2]^{1/2}$; $w = 1/\sigma^2(|F_o|)$. ^{c} Quality-of-fit = $[\sum w(|F_o| - |F_c|)^2/(N_{obsd} - N_{parameters})]^{1/2}$.

Table III. Convergence R Factor and Equivalent Isotropic Thermal Parameters^a for Different Models of the Ortho-Metalated Pyridines Bridge System

		B, Å^2			
model^b	R, %	N1/CN1	N2/CN2	C5/NC5	C10/NC10
1	4.352	4.1 (4)	4.7 (4)	3.0 (4)	2.2 (3)
2	4.360	2.3 (3)	2.6 (3)	5.4 (4)	4.2 (4)
3	4.347	3.2 (3)	3.8 (4)	4.1 (4)	3.3 (4)
4	4.345	2.9 (3)	4.0 (4)	3.8 (4)	3.5 (4)

^{a} Defined as $^4/_3[a^2\beta_{11} + b^2\beta_{22} + c^2\beta_{33} + ab(\cos\gamma)\beta_{12} + ac(\cos\beta)\beta_{13} + bc(\cos\alpha)\beta_{23}]$. ^{b} See Experimental Section.

other two as $(1 - x)$N + xC so as to obtain a head-to-tail arrangement [i.e., one atom of one ring being xN + $(1 - x)$C, the atom of the other ring that is attached to the same iridium atom was $(1 - x)$N + xC]. The free variable x was refined together with the other parameters with the SHELX-76 package of programs and was found to converge to 0.37 (7). This can be designated an unconstrained, disordered HT model. Final R factors and thermal parameters for the four models are reported in Table III. The last model, which was the one refining to the lowest R value, was used to obtain fractional atomic coordinates (reported in Table IV) and bond distances and angles (Table V). The largest peak in the difference Fourier map (1.56 e·Å^{-3}) was located at 1.19 Å from Ir1, 1.36 Å from Ir2, and 1.82 Å from N2/CN2. The second largest peak had a height of 1.16 e·Å^{-3}. An unconstrained disordered HH model was also considered [i.e. with the two atoms on Ir1 treated as xN + $(1 - x)$C and the other two as $(1 - x)$N + xC] and the free variable x was found to converge to 1.01 (1), which corresponds to model 1.

Results

(a) Synthesis and NMR Characterization of Compound 3. The thermal reaction between compound **1** and pyridine produces the ortho-metalated compound **3**. The reaction goes through the pyridine adduct **2**, which is promptly formed at room temperature (see reaction 1). The dark red compound **2**, which was isolated from the room temperature reaction and crystallographically characterized, has been reported earlier.[1]

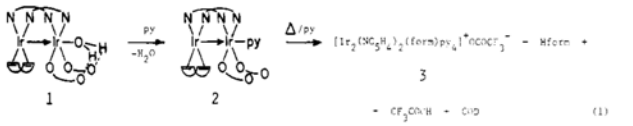

The structure of compound **3** has been deduced from analytical, IR, and ^{1}H, ^{13}C, and ^{19}F NMR data and further confirmed by X-ray crystallography. The presence of the uncoordinated trifluoroacetate anion, although not evident in the ^{13}C NMR spectrum (presumably because of long T_1 values for the corresponding carbon atoms), is substantiated by F analysis, by the carboxylate stretching vibration at 1690 cm^{-1} in the IR spectrum (cf. 1670 cm^{-1} in compound **1**)[1] and by the ^{19}F NMR singlet at −10.71 ppm (cf. −12.14 ppm for compound **1** in C_6D_6).[5] The presence of a bridging formamidinato group is shown by IR absorptions at 1580, 1540, and 1500 cm^{-1} (similar patterns were observed for **1**[1] and for $[Ir(\mu\text{-form})(COD)]_2$[6]) and by the methyl group resonances in the ^{1}H and ^{13}C{^{1}H} NMR spectra. Both these spectra indicate that there are two different types of methyl groups (δ_H 2.26 and 2.24 and δ_C 20.77 and 20.70; solvent = CD_2Cl_2). Integration of the proton spectrum indicates that we have one formamidinato group per dimer. This means that the two ends of the formamidinato ligand are magnetically different. The rest of the ^{1}H NMR spectrum consists of a complicated pattern in the aromatic region, and it is not very informative. It indicates, however, that the COD ligand is no longer present in the product of reaction 1. The ^{13}C{^{1}H} NMR spectrum also exhibits a complicated pattern in the aromatic region (see Table I), indicating a considerable number of different carbon atoms. A ^{13}C{APT} NMR analysis (APT = attached proton test)[7] (see Figure 1) provides further information. The spectrum of **3**-py in CD_2Cl_2 (Figure 1a) shows six different aromatic carbon atoms that are not attached to hydrogen atoms (peaks pointing downward). We would expect four such peaks for the ipso and para carbon atoms of the two different benzene rings of the formamidinato ligand, as suggested by the methyl resonances. A similar situation was found for compound **1**,[1] those resonances being at 145.98 and 145.85 ppm for the ipso C and at 135.75 and 135.29 ppm for the para C atoms. We therefore assign the peaks at 150.43 and 149.81 ppm to the ipso C and those at 133.44 and 133.06 ppm to the para C atoms of the formamidinato benzene rings in compound **3**. The other two peaks pointing downward (at 164.97 and 162.37 ppm) are assigned to ortho-metalated carbon atoms of as many pyridine rings. The low-field position of these resonances is consistent with metalation. Although quite a few ortho-metalated pyridine complexes have been reported, ^{13}C NMR data on them are scarce. The resonance of the ortho-metalated carbon in $(C_5Me_5)Lu(NC_5H_4)$ was found as far downfield as 234.26 ppm in C_6D_{12}.[8] The ^{13}C NMR spectrum of a series of Ru and Os trinuclear clusters containing ortho-metalated pyridine and other heteroaromatic amines have been reported,[9] but a clear assignment of the resonances due to the ortho-metalated carbon atoms was not possible.

(5) Unreported result from this laboratory.
(6) Cotton, F. A.; Poli, R. *Inorg. Chim. Acta* **1986**, *122*, 243.
(7) (a) Rabenstein, D. L.; Nakachima, T. T. *Anal. Chem.* **1979**, *51*, 1465A. (b) Lecocq, C.; Lallemand, J.-Y. *J. Chem. Soc., Chem. Comm.* **1981**, 150. (c) Patt, S. L.; Shoolery, J. N. *J. Magn. Reson.* **1982**, *46*, 535.
(8) Watson, P. L. *J. Chem. Soc., Chem. Commun.* **1983**, 276.
(9) Eisenstadt, A.; Giandomenico, C. M.; Frederick, M. F.; Laine, R. M. *Organometallics* **1985**, *4*, 2033.

Table IV. Atomic Positional Parameters and Equivalent Isotropic Displacement Parameters (Å²)[a] and Their Estimated Standard Deviations for $[Ir_2(\mu\text{-}NC_5H_4)_2(\mu\text{-form})(py)_2(MeCN)_2][BPh_4]\cdot 2MeCN$

atom	x	y	z	B	atom	x	y	z	B
Ir1	0.83246 (3)	0.85827 (3)	0.90787 (6)	3.13 (2)	C54	0.940 (1)	0.879 (1)	1.341 (2)	5.4 (6)
Ir2	0.76177 (3)	0.75306 (3)	0.88125 (6)	3.17 (2)	C55	0.8945 (9)	0.8912 (8)	1.215 (2)	4.7 (5)
N1[b]	0.7682 (7)	0.8639 (7)	0.722 (1)	2.9 (3)	C61	0.7945 (9)	0.7395 (8)	1.201 (2)	4.0 (4)
CN1[c]	0.7682 (7)	0.8639 (7)	0.722 (1)	2.9 (3)	C62	0.826 (1)	0.705 (1)	1.324 (2)	5.0 (5)
N2[c]	0.7335 (7)	0.8973 (8)	0.998 (1)	4.0 (4)	C63	0.874 (1)	0.6343 (9)	1.318 (2)	4.8 (5)
CN2[b]	0.7335 (7)	0.8973 (8)	0.998 (1)	4.0 (4)	C64	0.887 (1)	0.5977 (9)	1.187 (2)	5.4 (5)
N3	0.9201 (6)	0.7847 (6)	0.803 (1)	3.6 (3)	C65	0.856 (1)	0.6318 (9)	1.067 (2)	5.3 (5)
N4	0.8518 (7)	0.6878 (6)	0.773 (1)	3.4 (3)	C70	0.890 (1)	1.015 (1)	0.910 (2)	4.7 (5)
N5	0.9000 (7)	0.8387 (6)	1.102 (1)	3.7 (3)	C71	0.921 (1)	1.0842 (9)	0.901 (2)	7.0 (7)
N6	0.8088 (7)	0.7015 (6)	1.072 (1)	3.9 (3)	C80	0.638 (1)	0.6424 (9)	0.841 (2)	4.5 (5)
N7	0.8668 (7)	0.9620 (6)	0.915 (1)	4.3 (4)	C81	0.582 (1)	0.597 (1)	0.824 (2)	6.8 (6)
N8	0.6812 (7)	0.6812 (6)	0.853 (1)	4.1 (3)	N9	0.077 (1)	0.587 (1)	1.005 (3)	9.9 (8)
C1	0.7644 (9)	0.9098 (9)	0.615 (2)	4.5 (5)	C90	0.140 (2)	0.560 (1)	1.039 (3)	9 (1)
C2	0.7158 (9)	0.8972 (9)	0.490 (2)	5.1 (5)	C91	0.222 (1)	0.528 (1)	1.083 (3)	11 (1)
C3	0.6709 (9)	0.8431 (9)	0.478 (2)	4.6 (5)	N10	0.867 (1)	1.049 (1)	1.555 (2)	9.0 (7)
C4	0.6767 (8)	0.7975 (8)	0.591 (2)	4.0 (4)	C100	0.802 (2)	1.086 (1)	1.557 (2)	7.5 (8)
C5[c]	0.7280 (8)	0.8077 (7)	0.711 (1)	3.8 (4)	C101	0.727 (1)	1.132 (1)	1.552 (2)	9.8 (8)
NC5[b]	0.7280 (8)	0.8077 (7)	0.711 (1)	3.8 (4)	C110	0.5885 (8)	0.2684 (8)	1.031 (2)	4.3 (4)
C6	0.702 (1)	0.9678 (8)	1.070 (2)	4.8 (5)	C111	0.552 (1)	0.2230 (9)	1.091 (2)	5.0 (5)
C7	0.630 (1)	0.976 (1)	1.123 (2)	6.1 (6)	C112	0.555 (1)	0.223 (1)	1.238 (2)	6.0 (6)
C8	0.591 (1)	0.918 (1)	1.110 (2)	5.5 (6)	C113	0.594 (1)	0.273 (1)	1.326 (2)	6.9 (7)
C9	0.6260 (8)	0.8485 (9)	1.037 (2)	4.0 (4)	C114	0.631 (1)	0.321 (1)	1.269 (2)	6.6 (6)
C10[b]	0.6936 (7)	0.8397 (6)	0.985 (1)	3.5 (4)	C115	0.630 (1)	0.3178 (9)	1.120 (2)	5.3 (5)
NC10[c]	0.6936 (7)	0.8397 (6)	0.985 (1)	3.5 (4)	C120	0.6541 (8)	0.2937 (8)	0.803 (2)	3.8 (4)
C11	0.9118 (9)	0.7150 (8)	0.753 (2)	3.6 (4)	C121	0.7285 (9)	0.2614 (9)	0.861 (2)	4.6 (5)
C30	0.9909 (9)	0.8003 (8)	0.782 (1)	3.5 (4)	C122	0.795 (1)	0.273 (1)	0.810 (2)	6.1 (6)
C31	1.0609 (8)	0.7503 (8)	0.826 (2)	3.7 (4)	C123	0.788 (1)	0.315 (1)	0.696 (2)	6.6 (6)
C32	1.134 (1)	0.768 (1)	0.815 (2)	5.2 (5)	C124	0.713 (1)	0.348 (1)	0.639 (2)	6.0 (6)
C33	1.135 (1)	0.8369 (9)	0.767 (2)	4.5 (5)	C125	0.648 (1)	0.3357 (9)	0.692 (2)	5.2 (5)
C34	1.0648 (9)	0.8854 (8)	0.723 (2)	3.8 (4)	C130	0.5722 (8)	0.1903 (8)	0.771 (2)	4.2 (4)
C35	0.9926 (9)	0.8679 (8)	0.731 (1)	3.7 (4)	C131	0.6107 (8)	0.1230 (9)	0.826 (2)	4.5 (4)
C36	1.213 (1)	0.858 (1)	0.775 (2)	6.7 (6)	C132	0.609 (1)	0.0523 (9)	0.747 (2)	5.5 (5)
C40	0.851 (1)	0.6146 (8)	0.694 (1)	3.8 (4)	C133	0.569 (1)	0.0498 (9)	0.616 (2)	5.3 (5)
C41	0.7853 (9)	0.6027 (8)	0.608 (2)	4.1 (5)	C134	0.533 (1)	0.117 (1)	0.558 (2)	5.5 (5)
C42	0.7881 (9)	0.5339 (8)	0.525 (2)	4.4 (5)	C135	0.5331 (8)	0.1860 (8)	0.633 (2)	4.2 (4)
C43	0.854 (1)	0.4783 (8)	0.525 (2)	4.5 (5)	C140	0.5009 (9)	0.3375 (8)	0.828 (1)	4.1 (4)
C44	0.921 (1)	0.4886 (9)	0.615 (2)	5.4 (5)	C141	0.426 (1)	0.3226 (9)	0.799 (2)	4.9 (5)
C45	0.9190 (9)	0.5578 (8)	0.704 (2)	4.1 (4)	C142	0.358 (1)	0.380 (1)	0.782 (2)	5.8 (6)
C46	0.860 (1)	0.4047 (9)	0.424 (2)	7.0 (6)	C143	0.367 (1)	0.455 (1)	0.797 (2)	5.6 (5)
C51	0.9520 (8)	0.7732 (9)	1.116 (2)	3.7 (4)	C144	0.439 (1)	0.473 (1)	0.830 (2)	6.1 (6)
C52	0.9991 (9)	0.7574 (9)	1.242 (2)	4.6 (5)	C145	0.504 (1)	0.4151 (9)	0.846 (2)	5.7 (6)
C53	0.994 (1)	0.814 (1)	1.358 (2)	5.5 (5)	B	0.579 (1)	0.2717 (9)	0.855 (2)	4.1 (5)

[a] Anisotropically refined atoms are given in the form of the equivalent isotropic displacement parameter defined as $^4/_3[a^2\beta_{11} + b^2\beta_{22} + c^2\beta_{33} + ab(\cos\gamma)\beta_{12} + ac(\cos\beta)\beta_{13} + bc(\cos\alpha)\beta_{23}]$. [b] Site occupancy factor = 0.37 (7) [c] Site occupancy factor = 0.63 (7).

Table V. Selected Bond Distances (Å) and Angles (deg) and Their Estimated Standard Deviations for $[Ir_2(\mu\text{-}NC_5H_4)_2(\mu\text{-form})(py)_2(MeCN)_2][BPh_4]\cdot 2MeCN$[a]

atom 1	atom 2	dist	atom 1	atom 2	dist	atom 1	atom 2	dist
Ir1	Ir2	2.518 (1)	Ir2	N4	2.097 (11)	N2/CN2	C10/NC10	1.39 (2)
Ir1	N1/CN1	2.003 (11)	Ir2	N6	2.160 (12)	N3	C11	1.35 (2)
Ir1	N2/CN2	2.024 (12)	Ir2	N8	2.143 (13)	N4	C11	1.33 (2)
Ir1	N3	2.107 (11)	Ir2	C5/NC5	1.983 (13)	N7	C70	1.14 (2)
Ir1	N5	2.114 (10)	Ir2	C10/NC10	2.019 (11)	N8	C80	1.15 (2)
Ir1	N7	2.126 (12)	N1/CN1	C5/NC5	1.38 (2)			

atom 1	atom 2	atom 3	angle	atom 1	atom 2	atom 3	angle	atom 1	atom 2	atom 3	angle
Ir2	Ir1	N1/CN1	73.4 (4)	N3	Ir1	N7	101.1 (5)	N6	Ir2	C10	92.3 (5)
Ir2	Ir1	N2/CN2	72.5 (4)	N5	Ir1	N7	89.1 (5)	N8	Ir2	C5/NC5	99.9 (5)
Ir2	Ir1	N3	88.1 (3)	Ir1	Ir2	N4	87.5 (3)	N8	Ir2	C10/NC10	95.4 (5)
Ir2	Ir1	N5	100.4 (4)	Ir1	Ir2	N6	100.0 (3)	C5/NC5	Ir2	C10/NC10	87.1 (5)
Ir2	Ir1	N7	166.8 (3)	Ir1	Ir2	N8	168.4 (3)	Ir1	N1/CN1	C5/NC5	105.7 (9)
N1/CN1	Ir1	N2/CN2	87.4 (5)	Ir1	Ir2	C5/NC5	73.2 (4)	Ir1	N2/CN2	C10/NC10	108.5 (8)
N1/CN1	Ir1	N3	87.3 (4)	Ir1	Ir2	C10/NC10	75.2 (4)	Ir1	N3	C11	120 (1)
N1/CN1	Ir1	N5	173.2 (5)	N4	Ir2	N6	91.9 (4)	Ir2	N4	C11	121.2 (8)
N1/CN1	Ir1	N7	97.4 (5)	N4	Ir2	N8	101.6 (4)	Ir1	N7	C70	174 (1)
N2/CN2	Ir1	N3	160.5 (5)	N4	Ir2	C5/NC5	86.8 (5)	Ir2	N8	C80	178 (1)
N2/CN2	Ir1	N5	93.5 (4)	N4	Ir2	C10/NC10	162.6 (5)	Ir2	C5/NC5	N1/CN1	107.6 (9)
N2/CN2	Ir1	N7	98.1 (5)	N6	Ir2	N8	87.0 (5)	Ir2	C10/NC10	N2/CN2	103.9 (9)
N3	Ir1	N5	89.7 (4)	N6	Ir2	C5/NC5	173.2 (6)	N3	C11	N4	123 (1)

[a] Numbers in parentheses are estimated standard deviations in the least significant digits.

However, the authors suggest[9] that these resonances are in the same region as the carbonyl carbon resonances, i.e., between 160 and 200 ppm.

The fact that we observe two resonances for the ortho-metalated carbon atoms in compound **3** is consistent with our formulation, since the two metalated pyridine groups

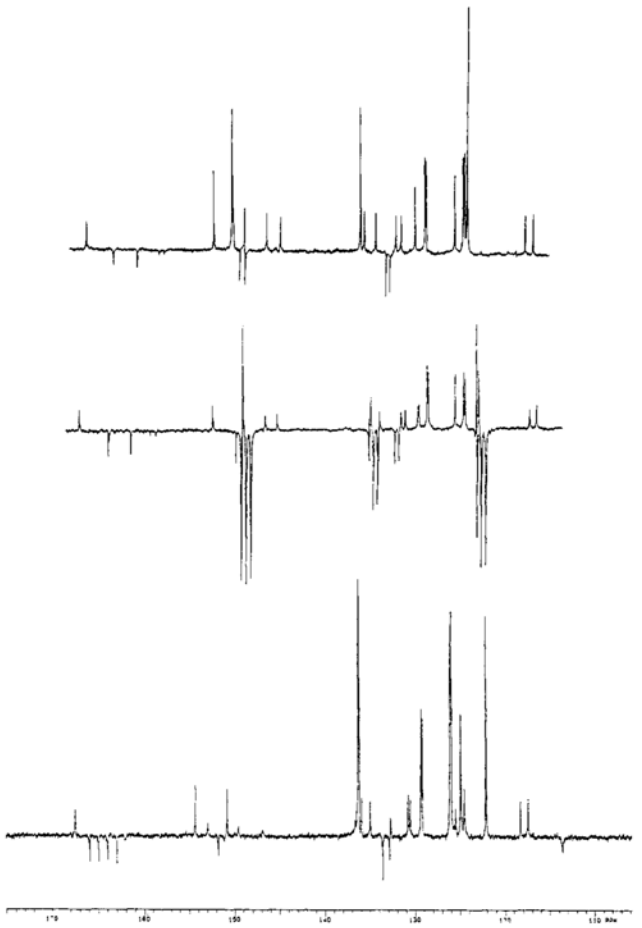

Figure 1. ^{13}C-attached proton test NMR spectra (T = 20 °C): (a) 3·py/CD_2Cl_2; (b) 3·py/py-d_5; (c) 4·2MeCN/CD_2Cl_2.

are trans to different ligands. This result, however, does not allow us to discriminate between the two possible orientations, i.e., head-to-head (A) and head-to-tail (B), since both have one carbon atom trans to the formamidinato bridge and the other trans to a pyridine group. The inequivalence of the two ends of the formamidinato ligand is also consistent with either isomeric form. The ^{13}C NMR spectra clearly show, however, that *only one of the two isomers is present.*

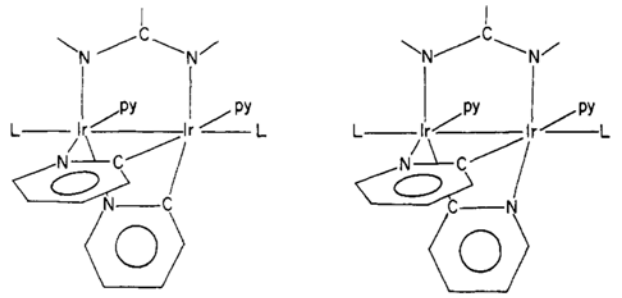

A

B

There are two additional very weak peaks due to carbon atoms not attached to protons, at 160.15 and 159.54 ppm, almost confused in the base-line noise (see Figure 1a). They might possibly be the internal peaks of a quartet due to the carbonyl carbon atom of the trifluoroacetate anion. Their separation corresponds to 30.7 Hz (in compound 1, the trifluoroacetate carbonyl carbon resonates at 170.68 ppm, with J_{C-F} = 37.3 Hz).[1] No peak attributable to the CF_3 carbon atom was found.

The *C*H resonance at 168.09 ppm is assigned to the formamidinato carbon atom (cf. 165.03 ppm for compound 1).[1] None of the other peaks can be assigned with absolute certainty, but a few highly probable assignments can be made. The ortho and meta carbon atoms of the formamidinato benzene rings should give rise to a set of two close peaks each, as found for compound 1. Resonances there were found[1] at 129.61 and 129.46 ppm for the ortho and at 126.69 and 125.77 pm for the meta carbon atoms. We find sets of two peaks in similar positions for compound 3 (129.33 and 129.22 ppm for ortho and 125.26 and 125.12 ppm for meta). The second set is very close to a third peak at 125.00 ppm, but, unlike the latter, this set is relatively unaffected by changing solvent and/or counterion (vide infra).

Compound 3·py contains uncoordinated pyridine as well as pyridine ligands in the axial and equatorial positions. We then expect to see three peaks for the free pyridine, whose intensity may be particularly high if this exchanges with at least some of the coordinated ones. We actually see three intense peaks at 151.36, 136.33, and 124.69 ppm. They are assigned to the ortho, para, and meta carbon atoms, respectively, by comparison with literature data.[10] It will be shown later that the axial pyridine ligands are labile while the equatorial ones are not. These three peaks are therefore assigned to the combination of free and axial pyridine molecules that are in rapid exchange.

Fourteen more peaks would be expected for the rest of the aromatic carbon atoms of the molecule (for either A or B isomer), consisting of the ortho, meta, and para atoms of the two inequivalent equatorial pyridine ligands and the 3-, 4-, 5-, and 6-carbon atoms of the two inequivalent ortho-metalated pyridine groups. We actually observe 13 more peaks in the spectrum of Figure 1a. Furthermore, when we finally take the same spectrum in C_5D_5N as solvent, one of the peaks (at 130.41 ppm) splits up into two peaks at 130.62 and 130.56 ppm to give the expected number of resonances (see Figure 1b). On the basis of the relative position and intensity (assuming a similar relaxation time for all the C–H-type carbon atoms of pyridine and ortho-metalated pyridine groups) we can assign the peaks at 153.42 and 149.97 ppm to the ortho carbon atoms of the equatorial pyridine ligands and those at 126.05 and 125.00 ppm to the meta carbon atoms of the same groups. The remaining two weaker peaks in the region of pyridine ortho carbons (at 147.56 and 146.04 ppm) may be assigned to the 6-C of the ortho-metalated pyridine rings. Only the para C of the equatorial pyridine ligands and the 3-, 4-, and 5-C of the two ortho-metalated pyridine rings remain to be assigned, and this is not possible without additional data, as for example spectra of substituted pyridine derivatives.

(b) X-ray Crystal Structure of Compound 3. Compound 3 has been subjected to a crystal structure determination. The results obtained confirm the structure observed in solution (vide supra) for the cation. However, neither the trifluoroacetate anion nor the interstitial pyridine molecule could be clearly recognized, presumably because of disorder and/or high thermal motion. The structure could not therefore be refined below a figure of 8.8% for the agreement factor R. A view of the cation is shown in Figure 2. The compound crystallizes in the monoclinic space group $P2_1/n$, and no symmetry is imposed on the molecule.

The incomplete refinement of this structure caused by the disorder of the anion and the interstitial pyridine makes the distances and angles relatively inaccurate. Since we have a more accurate structure for a closely related

(10) Gordon, A. J.; Ford, R. A. *The Chemist's Companion*; Wiley: New York, 1972 and references therein.

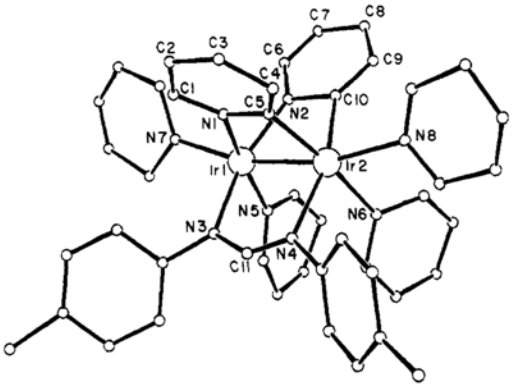

Figure 2. An ORTEP view of the diiridium cation in compound **3**·py. Nitrogen and carbon atoms have been drawn with arbitrary radii for the sake of clarity.

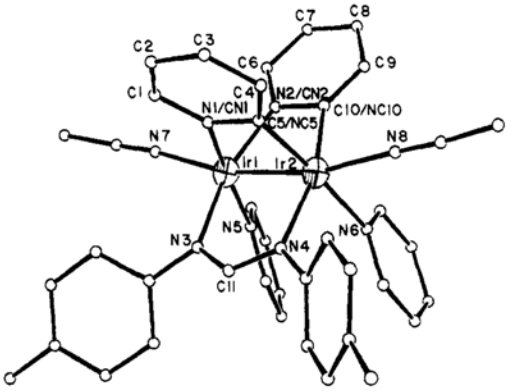

Figure 3. An ORTEP view of the diiridium cation in compound **4**·2MeCN. Nitrogen and carbon atoms have been drawn with arbitrary radii for the sake of clarity.

dinuclear cation from the crystallographic study of compound **4**, the bond lengths and angles of **3** are not tabulated. In general, the comparable dimensions are very similar in the two cases.

(c) Synthesis and NMR Spectroscopic Characterization of Compound 4. Although the formulation of compound **3** as $[Ir_2(\mu\text{-}NC_5H_4)_2(\mu\text{-form})(py)_4]^+ OCOCF_3^-\cdot py$ is convincing from the combined analytical, spectroscopic, and crystallographic data presented above, we decided to perform an ion metathesis on compound **3**, the goal being the preparation of a salt with an anion that could be crystallographically (and spectroscopically) better determined.

Interaction of compound **3** with $NaBPh_4$ in MeCN as solvent resulted in the crystallization of **4**·2MeCN upon cooling to −20 °C (see reaction 2).

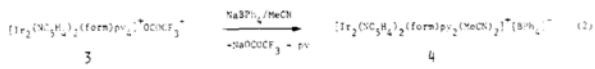

3 4 (2)

Acetonitrile has replaced pyridine in the axial position of the diiridium cation in the course of the ion metathesis reaction. This is indicated by combined analytical and NMR data and confirmed by the crystal structure determination (vide infra). The ^{1}H-NMR spectrum shows the formamidinato methyl proton resonances at 2.38 and 2.31 ppm, again indicating magnetically different ends of the formamidinato ligand. There is, in addition, a single peak in the methyl region at 2.03 ppm corresponding to 12 protons, assigned to four molecules of acetonitrile. Since the two axial acetonitrile ligands are in a different chemical environment with respect to the free MeCN (and with respect to each other for isomer A), this again means that the axial ligands are labile on the NMR time scale. Exchange must be, on the other hand, extremely slow in the equatorial positions, since compound **4** retains its equatorial pyridine ligands during its synthesis from **3**. Also, no exchange of the equatorial pyridine ligands was observed in the ^{13}C NMR spectrum of compound **3** when recorded in pure pyridine-d_5 (see Figure 1b). The rest of the ^{1}H NMR spectrum of **4**·2MeCN expectedly consists of a very complicated and therefore rather uniformative pattern in the aromatic region. The $^{13}C\{^1H\}$ NMR spectrum was recorded in CD_2Cl_2; it is reported in Table IV and compared with that of compound **3**. The BPh_4^- anion shows peaks at 164.37 (ipso C, J_{C-B} = 49.3 Hz), 136.20 (ortho C, J_{C-B} = 1.5 Hz), 125.98 (meta C, J_{C-B} = 2.7 Hz), and 122.06 ppm (para C). The J_{C-B} for the latter is estimated to be smaller than 1 Hz, which was the instrument resolution in our conditions. The values agree well with others reported in the literature.[11] The formamidinato methyl carbon resonances show up at 20.87 and 20.75 ppm, while the methyl carbon atoms of the rapidly exchanging axial and free acetonitrile ligands give rise to a single peak at 2.96 ppm. The cyano carbon atoms of the same groups give another single peak at 113.56 ppm which, in agreement with the absence of attached protons, is pointing downward in the ^{13}C(APT) NMR spectrum (shown in Figure 1c). The rest of the ^{13}C NMR spectrum agrees generally with that of compound **3**, therefore indicating that the core of the cation, consisting of the metal atoms, the bridging ligands, and the equatorial ligands, is the same for the two compounds, including the relative orientation of the ortho-metalated pyridine rings. The only major difference in the carbon NMR spectra of the two compounds is the weaker intensity of some of the peaks for compound **4**, although this spectrum was measured with about double the acquisition time with respect to the spectrum of **3**. The peak at 152.94 ppm cannot be assigned to any of the carbon atoms of compound **4**·2MeCN and is in the same position where the ortho carbon atom of pyridine (free + axial) was found for compound **3**. We believe this is due to some free pyridine cocrystallized with compound **4**·2MeCN, coming from the axial and free pyridine of **3**-py, although we cannot exclude a priori that some acetonitrile–*eq*-pyridine ligand exchange takes place.

(d) X-ray Crystal Structure of Compound 4. Compound **4**·2MeCN crystallizes in the triclinic space group $P\bar{1}$ with the molecule in a general position. The entire molecule was successfully refined without disorder problems, in contrast to compound **3**. The BPh_4^- anion and the interstitial MeCN molecules exhibit normal molecular geometries and need not be discussed further. Bond distances and angles related to them can be found in the supplementary material.

The geometry of the cation is illustrated in Figure 3 with the atomic numbering scheme employed, which corresponds to that used for compound **3**. The metal–metal distance, 2.518 (1) Å, is the shortest ever reported for an iridium–iridium single bond, although only slightly shorter than that recently found in the homoleptic Ir(II) dimer $Ir_2(form)_4$ [2.524 (3) Å].[12] The diiridium core is surrounded by three bridging ligands (one formamidinato and two ortho-metalated pyridine groups) and two equatorial pyridine ligands for both compounds **3** and **4**, the coordination sphere being completed by axial ligands (pyridine for **3** and acetonitrile for **4**).

(11) Mann, B. E.; Taylor, B. F. *^{13}C-NMR Data For Organometallic Compounds*; Academic: New York, 1981.
(12) Cotton, F. A.; Poli, R. *Polyhedron* **1987**, *6*, 1625.

The four distances between the iridium atoms and the atoms of the ortho-metalated pyridines that are attached to them are equivalent. These are therefore not useful for discerning the distribution of N and C atoms on these four sites. A similar situation was found for other ortho-metalated pyridine structures.[13-16] We approached this problem by refining different models as described in the Experimental Section and watching the variations in the *R* factor and in the thermal parameters of the atoms involved. The results obtained suggest a disordered structure with the four light atoms having mixed N and C character (37 and 63% in a head-to-tail model). However, since the difference between a nitrogen and a carbon atom is only one electron, this result is of doubtful significance. Also, a 50–50 disorder model, which is not so far from the figure obtained in the best refined model, is consistent with both the head-to-head and the head-to-tail model. We conclude that this aspect of the crystallographic results cannot distinguish between the two different isomeric forms (A and B) for compounds **3** and **4**.

The iridium–nitrogen distances in **4** are slightly longer for the equatorial pyridines [2.11 (1) and 2.16 (1) Å] and formamidinato bridge [2.11 (1) and 2.10 (1) Å] than for the ortho-metalated pyridine bridges [average 2.01 (1) Å]. This may be dictated by the requirements of the two-atom bridges. The iridium–nitrogen distances for the axial acetonitrile groups are comparable with the former [2.13 (1) and 2.14 (1) Å].

The four equatorially bonded atoms (N1/CN1, N2/CN2, N3, and N5 for Ir1 and C5/NC5, C10/NC10, N4, and N6 for Ir2) are in a distorted square-planar configuration, the metal atoms being displaced away from the plane by 0.238 (1) Å for Ir1 and 0.208 (1) Å for Ir2. These two planes deviate by 30.5 (5)° from being parallel, and the corresponding ligands are eclipsed when viewed along the iridium–iridium vector [average torsional angle is 0.7 (5)°]. The least-squares planes passing through the metals and each pair of related equatorial donor atoms form angles close to 90° between each other [92.0 (3), 90.1 (3), 90.3 (3), and 92.2 (3)° between N1–C5 and N2–C10, then continuing anticlockwise back to N1–C5 (see Figure 3)]. C11, the central carbon atom of the form ligand, is only 0.03 (1) Å out of the least-squares plane determined by Ir1, Ir2, N3, and N4, and the N3–C11 and N4–C11 bond lengths are identical within the experimental error [1.35 (2) and 1.33 (2) Å, respectively]. The other geometrical features are normal and do not require further comment.

Discussion

Reaction 1 can be considered a peculiar one for many reasons. First of all, it affords a product containing bridging ortho-metalated pyridine groups across a metal–metal bonded dimer. Very few other examples of this type of compound have been previously reported, e.g., $Os_2(\mu\text{-}NC_5H_4)(CO)_6$ (two isomers),[17] $[Pd(\mu\text{-}NC_5H_4)Br(PPh_3)]_2$,[13] and $Re_2(\mu\text{-}H)(\mu\text{-}NC_5H_4)(CO)_8$,[14] and none was known for iridium. A few compounds containing ortho-metalated pyridine and substituted pyridines spanning metal–metal bonds in higher nuclearity clusters are also known.[9,15] Second, the displacement of a very weakly acidic proton such as that bonded to the pyridine ortho carbon to produce much stronger acids such as formamidine and CF_3COOH is not an expected occurrence. The formation of the new bridges across the metal–metal bond must of course contribute substantially to the driving force for the reaction. This sort of reactivity was also observed in the interaction of **1** with HForm,[12] where Hform replaced the coordinated CF_3COO groups to produce CF_3COOH and the homoleptic quadruply bridged $Ir_2(form)_4$, but here the contrast between the weakness of the entering acid and the strength of the one displaced is less.

Scheme I

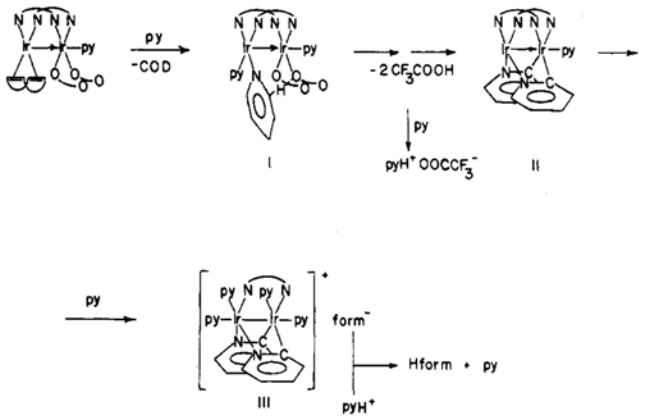

A determination of whether the dinuclear cation has a head-to-head (HH) or head-to-tail (HT) arrangement of the ortho-metalated pyridine ligands has been the most difficult part of this study. Let us recapitulate what we have learned (and also what can and cannot be learned) from spectroscopic studies. First, the NMR results tell us that we are dealing with only one isomer (or at least 95%). Second, the NMR results do not, or cannot, tell us which isomer that is. Both the HH and HT isomers have inequivalent equatorial pyridine ligands and inequivalent tolyl groups on the formamidinato ligand. Only by determining whether the iridium atoms, or the axial ligands, are equivalent or inequivalent could we tell whether the cation has the HH or HT structure. Such determinations appear to face insuperable problems. The most fundamental one is that a failure to detect such inequivalencies can never *prove* that there is an HT structure, since it could always be argued that differences exist but cannot be resolved. In addition there are several other problems. NMR studies cannot be carried out on iridium because of its high nuclear quadrupole moment and low sensitivity. NMR studies on the CH_3CN molecules are not helpful because they are very labile and appear equivalent for that reason alone. NMR studies on the solid substance would be of no use because the pairs of Ir atoms and the pairs of axial ligands are crystallographically inequivalent. Nuclear quadrupole resonance studies on the iridium nuclei might be feasible (although this is not likely), but this would require that they have very different field gradients to be proven inequivalent.

One possible way to obtain a chemical solution to the problem is to prepare an analogous complex using a substituted pyridine. This approach would also be fruitless if the iridium dimers with ortho-metalated substituted pyridines are disordered but could succeed if an ordered crystal structure is formed. We have been trying to do this by employing 4-methylpyridine, but so far the product has

(13) Nakatsu, K.; Kinoshita, K.; Kanda, H.; Isobe, K.; Nakamura, Y.; Kawaguchi, S. *Chem. Lett.* **1980**, 913.
(14) (a) Gard, D. R.; Brown, T. L. *Organometallics* **1982**, *1*, 1143. (b) Nubel, P. O.; Wilson, S. R.; Brown T. L. *Organometallics* **1983**, *2*, 515.
(15) (a) Jackson, P. F.; Johnson, B. F. G.; Lewis, J.; Nelson, W. J. H.; McPartlin, M. *J. Chem. Soc., Dalton Trans.* **1982**, 2099. (b) Deeming, A. J.; Peters, R.; Hursthouse, M. B.; Backer-Dirks, J. D. J. *J. Chem. Soc., Dalton Trans.* **1982**, 787. (c) Burgess, K.; Holden, H. D.; Johnson, B. F. G.; Lewis, J.; Hursthouse, M. B.; Walker, N. P. C.; Deeming, A. J.; Manning, P. J.; Peters, R. *J. Chem. Soc., Dalton Trans.* **1985**, 85.
(16) Thompson, M. E.; Bercaw, J. E. *Pure Appl. Chem.* **1984**, *56*, 1.
(17) Yin, C. C.; Deeming, A. J. *J. Chem. Soc., Dalton Trans.* **1975**, 2091.

Scheme II

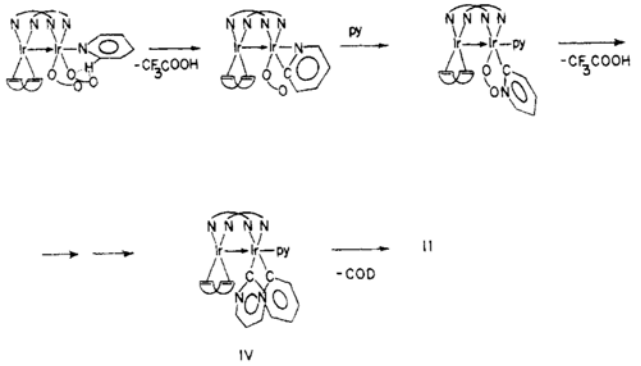

Scheme III

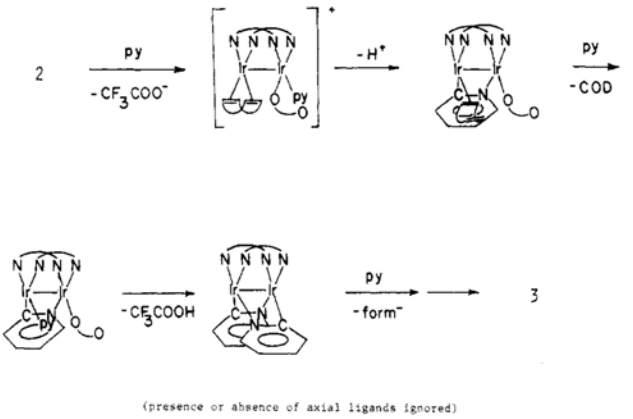

failed to form satisfactory crystals. We shall continue to pursue this approach, but in the meantime we think the results merit publication.

We have given some consideration to reasonable mechanisms for reaction 1. Three likely possibilities are shown in Schemes I–III, which may not, of course, be the only reasonable ones. We have already commented on the possible intermediacy of compound **2**. According to the first mechanism (Scheme I), the COD ligand in compound **2** would be replaced by pyridine molecules in the first step. The equatorial pyridine ligands in intermediate I would then undergo the ortho-metalation process with extrusion of CF_3COOH to afford intermediate II. At this point, most probably because of excessive strain caused by the bridge system (evident from the geometric parameters of compound **4**), one formamidinato group is replaced by pyridine ligands to produce III which, in turn, is transformed into the trifluoroacetate salt because of the higher basicity of the $[form]^-$ anion relative to py. In Scheme II, on the other hand, the ortho metalation takes place in the first step on the Ir(III) center to give a chelating NC_5H_4 ligand. Three-center metal–N–C rings with ortho-metalated pyridines have been reported before for other metals, e.g., Ti,[18] Lu,[8] and Sc.[16] Intermediate IV would be eventually obtained and would then undergo transformation into the intermediate II of Scheme I by elimination of COD. Both mechanisms would therefore lead to the HH isomer. Scheme III, on the other hand, shows a mechanism that leads to a HT isomer. The intermediate with the dangling COD ligand would be susceptible to attack at that iridium atom.

On mechanistic grounds, the formation of either an HH or HT isomer could be rationalized. Moreover, whichever isomer is the initial, kinetically controlled product could, if it is not the thermodynamically favored isomer, rearrange. Such isomerizations, in the direction of HH to HT isomers, at any rate, have been reported for a number of dinuclear systems containing pairs of unsymmetrical bridging ligands bound to pairs of platinum-group metal atoms.[17,19]

To sum up the present position regarding which isomer has been obtained, we believe that the X-ray crystallographic results favor the HT isomer, but they cannot be said to rule out the HH isomer, and there is no other evidence (e.g., spectroscopic) or line of reasoning (e.g., mechanistic) that can be used to make an unambiguous choice.

The bonding description of compounds **3** and **4** presents some interesting aspects, especially when contrasted with those given for compounds **1** and **2** and for $Ir_2(form)_4$.[12] Compounds **1** and **2** were described as mixed-valence Ir(I)–Ir(III) compounds containing a dative metal–metal bond. This description allows an electron count of 16 for Ir(I) and 18 for Ir(III), known to be typical for those oxidation states. The alternative Ir(II)–Ir(II) description with a covalent metal–metal bond was regarded as less plausible because of the different coordination spheres of the two iridium centers. In addition, homogeneous-valence Ir(II) dimers typically exhibit a pentacoordination completed by the formation of the metal–metal bond to give an 18e count for both metals. For these reasons we prefer to describe compounds **3** and **4**, differently to **1** and **2**,[1] and similarly to $Ir_2(form)_4$,[12] as homogeneous-valence Ir(II) dimers. We may note that this argument is in favor of the HT arrangement of the bridging ortho-metalated pyridine groups but does not demand it, since examples of homogeneous-valence HH compounds are known.[20]

Compounds **3** and **4** differ from $Ir_2(form)_4$ by the presence of axial ligands. The coordination of axial ligands is prevented in $Ir_2(form)_4$ by steric hindrance caused by four tolyl groups around each axial site.[12] The same situation was found for $Rh_2(form)_4$.[21] In compounds **3** and **4**, on the other hand, the axial positions are easily accessible. Comparison of the metal–metal distances in **4** and $Ir_2(form)_4$[12] indicates that axial coordination does not have a profound effect on the Ir–Ir bond length. In other metal–metal bonded compounds, including those of rhodium,[22] the axial ligation generally causes some lengthening of the metal–metal bond. Of course, the bridging system is different in the two cases, and it may be that the less flexible two-atom-bridging pyridine groups force the two iridium atoms closer to each other. Although the iridium–nitrogen distances are comparable for axial and equatorial ligands, the axial ligands are much more labile and rapidly exchange on the NMR-time scale. This behavior is identical with that observed for rhodium(II) dinuclear complexes.[22]

To summarize, compound **1** has been found to activate the ortho C–H bond of pyridine to afford bis(ortho-metalated pyridine)-bridged Ir(II) dimers that belong to the class of d^7 dimers with a single metal–metal bond of $\omega^2\pi^4\delta^2\delta^{*2}\pi^{*4}$ electronic configuration. Compound **1** and

(18) Klei, E.; Teuben, J. H. *J. Organomet. Chem.* **1981**, *214*, 53.
(19) (a) Farr, J. P.; Wood, F. E.; Balch, A. L. *Inorg. Chem.* **1983**, *22*, 3387. (b) O'Halloran, T. V.; Lippard, S. J. *J. Am. Chem. Soc.* **1983**, *105*, 3341.
(20) (a) Cotton, F. A.; Felthouse, T. R. *Inorg. Chem.* **1981**, *20*, 584. (b) Cotton, F. A.; Falvello, L. R.; Han, S.; Wang, W. *Inorg. Chem.* **1983**, *22*, 4106.
(21) Piraino, P.; Bruno, G.; Lo Schiavo, S.; Laschi, F.; Zanello, P. *Inorg. Chem.*, in press.
(22) (a) Cotton, F. A.; Walton, R. A. *Multiple Bonds Between Metal Atoms*, Wiley: New York, 1982. (b) Cotton, F. A.; Walton, R. A. *Metal-metal Multiple Bonds in Dinuclear Clusters*, *Struct. Bonding (Berlin)* **1985**, *62*, 1.

its derivatives are potentially useful starting materials for organometallic chemistry and catalysis on a diiridium center.

Acknowledgment. We thank the National Science Foundation for support of this work and Miss Viji Dandapani for the ^{19}F NMR spectroscopic measurements.

Registry No. 1, 106682-12-6; 3, 109011-40-7; 3·pg, 109011-41-8; 4, 109011-43-0; 4·2MeCN, 109011-44-1.

Supplementary Material Available: Tables of bond distances and angles and a listing of anisotropic displacement parameters for compound 4 and a table of fractional atomic coordinates and isotropic displacement parameters for compound 3 (11 pages); a table of observed and calculated structure factors for compound 4 (23 pages). Ordering information is given on any current masthead page.